13

Metalorganic vapor phase epitaxy of AlN layers on a nanostructured AlN/Si(100) template synthesized by reactive magnetron sputtering

© V.N. Bessolov,[1] M.E. Kompan,[1] E.V. Konenkova,[1] T.A. Orlova,[1] S.N. Rodin,[1] A.V. Solomnikova[2]

[1] Ioffe Institute,
St. Petersburg, Russia
[2] St. Petersburg State Electrotechnical University
„LETI“, St. Petersburg, Russia
e-mail: lena@triat.mail.ioffe.ru

Received December 4, 2023
Revised April 23, 2024
Accepted April 25, 2024

The atomic force microscopy and Raman scattering methods were used to study AlN layers grown by metalorganic vapor phase epitaxy (MOCVD) on a Si(100) substrate, on the surface of which a symmetrical V-shaped nanostructure with an element size < 100 nm (NP-Si(100) substrate) and an AlN buffer layer obtained by the method of reactive magnetron sputtering (RMS). It is shown that during the formation of the buffer layer at the initial stage of growth, a transition from the symmetrical state of the structured substrate to the asymmetric state of the layer is carried out. It was found that the buffer layer grown by RMS is in a state of compression, and the layer grown by MOCVD has a lower amount of stretching than the AlN layer obtained directly on the NP-Si(100) substrate. It is assumed that such textural buffer layers after RMS deposition contain hexagonal and cubic phases of AlN.

Keywords: aluminum nitride, nanostructured silicon substrate, reactive magnetron sputtering.

DOI: 10.61011/TP.2024.06.58830.296-23

Introduction

Recently AlN attracted significant attention owing to its superb properties and potential applications, such as ultraviolet diodes, acoustic resonant cavities and power electronic devices [1,2]. Growth of AlN layers on a Si(111)-substrate is preferable due to low cost and good availability of Si-substrates, their large surface area, high heat conductivity and prospects of integration of nitride-gallium and silicon electronics [3,4]. Si substrates may be easily removed by method of moist chemical etching [5].

However, it is rather hard to grow high-quality AlN on Si substrates. First, a large lattice mismatch ($\sim 19\%$) between AlN and Si(111) normally results in high densities of threading dislocations and an initial tension stress. Second, a huge mismatch between the coefficients of thermal expansion ($\sim 43\%$) of AlN and Si leads to additional tension stress in the process of cooling the structures from the growth temperature to room temperature [6]. Therefore, the thickness of AlN layers grown on Si, as a rule, was lower than $1\,\mu$m to prevent cracking, which was not sufficient to avoid penetration of dislocations from the heteroboundary and improvement of AIN quality.

The important physical property of III-nitrides with hexagonal crystalline structure consists in the fact that in heterostructures of these compounds the layers in direction along the axis of symmetry „c“ are characterized by the presence of piezoelectric polarization, which causes the inner electric field, leading to quantum-confined Stark effect [7], increased time for recombination of charge carriers [8] and lower optical gain [9].

If the growth plane of the layer is arranged at the angle to axis „c“, for example, as in GaN(10−11) or GaN(11−22), in this case semipolar crystals are formed with the reduced built-in electric field [10].

Semipolar layers GaN(11−22) were grown by method of reactive magnetron sputtering (RMS) on m-Al_2O_3-substrate at 800°C and after high temperature annealing at temperature 1600°C made it possible to obtain layers with width at half maximum of X-ray diffraction AlN 0.186°, 0.243° in direction [11−23] and [1−100] accordingly [11].

Recently RMS method heightens research interest in growing AlN on Si(111), since this is a simple method of epitaxy at low temperatures (around 400°C) [12] and even at room one [13]. It is expected that low growth temperature will give the advantage of RMS compared to other methods (gas phase epitaxy from metal-organic compounds (MOCVD), molecular-beam epitaxy) to obtain buffer layers at heteroepitaxy AlN on Si, since it makes it possible to lower mutual diffusion between Si and Al on heteroboundary [12].

The objective of this paper is to develop a new approach for coupling of the nanostructured substrate NP-Si(100) with hexagonal layer AlN at the expense of using low-temperature RMS method and low-temperature MOCVD method. We found no publications dedicated to growth of AIN layers by RMS method on silicon nanostructured substrates Si(100).

1. Experiment

RMS and MOCVD methods were used to growth three types of AlN layers on NP-Si(100) substrates noted as „A“, „B“, „C“: structure „A“ — AlN layer was grown with thickness 300 nm by MOCVD method, „B“ — RMS method was used to apply buffer AlN layer with thickness 60 nm, and then MOCVD method was used to grow AlN layer with thickness 300 nm, „C“ — used RMS method to only grow AlN layer with thickness 60 nm.

NP-Si(100) substrates were made using Wostec technology by etching in KOH solution similarly to [13] and had V-shaped nanogrooves, with the mean period of around 50 nm, height of ~ 40 nm (Fig. 1). Inclination angles of silicon slopes made around 55° (Si(111) faces). NP-Si(100) substrate underwent the standard cleaning procedure and was then etched in hydrofluoric acid aqueous solution. The process of application of a buffer AlN layer by RMS method took place in plasma mix N2/Ar at $T = 450°$C. MOCVD method was used to grow AlN layers on the modified plant EpiQuip with a horizontal reactor and an induction-heated graphite substrate holder similarly to [14].

Specimens were studied by methods of Raman scattering (RS) and atomic-force microscopy (AFM). RS was carried out using Raman spectrometer JY HORIBA MRS 320. The source of light was helium-neon laser with wavelength 632.8 nm. Investigations were conducted at a room temperature similarly to [15]. Measurements of specimen surface morphology were carried out using AFM in semicontact mode of measurements on a scanning probe microscope SolverNEXT similarly to [16].

2. Results

Image of AlN layer produced by RMS method shows that the layer grows in blocks, originating on the surface of Si(111) face, besides, structure of symmetrical surface NP-Si(100) turns into asymmetric surface of AlN layer (Fig. 1). Size of blocks in direction along the nanogroove is more than in the perpendicular one (Fig.1).

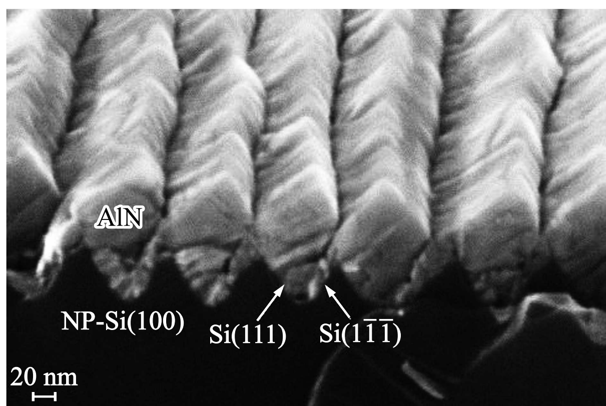

Figure 1. SEM images of AlN/NP-Si(100) structure after magnetron sputtering of AlN.

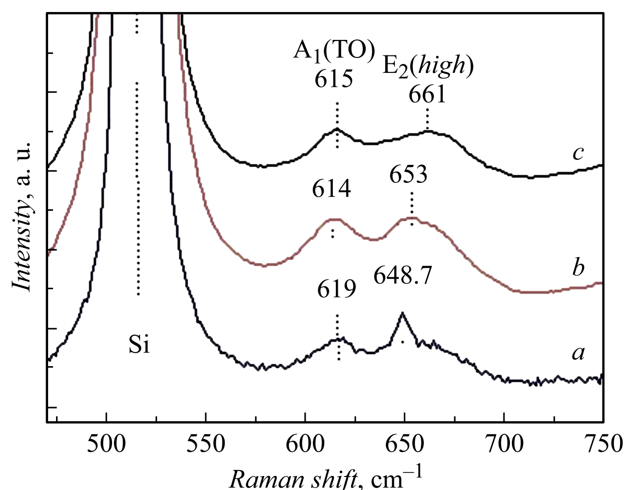

Figure 2. Spectra of RS AlN structures on NP-Si(100) substrate: *a* — type „A“, *b* — type „B“, *c* — type „C“.

RS spectra of AlN/Np-Si(100) for structures „A“, „B“ and „C“ after synthesis differed significantly (Fig. 2): for structure „A“ the peaks E_2(high) — 648.7 cm^{-1} and A_1(TO) — 619 cm^{-1} appeared, for structure „B“ — E_2(high) — 653.7 cm^{-1}, A_1(TO) — 614 cm^{-1} and for „C“ — peaks 661 cm^{-1} and 615 cm^{-1}. Synthesis of AlN layer by MOCVD method on a substrate with AlN buffer layer synthesized by RMS method (type „B“), shows lower tensile strain compared to structures of type „A“. As it is known, the peak position for unstrained AlN: E_2(high) — around 657.0 cm^{-1} [17]. You can see that the position of the peak on line E_2(high) for AlN layers is moved to the low-frequency side relative to its position in the non-deformed layer. This fact supports availability of tensile strain in AlN in plane parallel to the plane of the substrate, and shift wave indicates the residual strain value. Availability of tensile strains in AlN sublayers grown on Si(111), is easy to understand, if you take into account the fact that the lattice parameter for AlN is lower, and thermal expansion coefficient for AlN is higher than for Si(111), which causes deformation of the structure at epitaxy temperature and its increase when cooled down to room temperature. RS spectra for the structure only with AlN layer grown by RMS method contains peak 661 cm^{-1}, which characterizes the compression of the layer that may be related to manifestation of AlN cubic phase as noted in [18].

3. Results and discussion

In Fig. 1 you may find that the layer originates in several directions both on faces Si(111) and Si(1−1−1), and on the bottom of the groove Si(100). When AlN layers originate and grow on the nanostructured Si(100) surface,

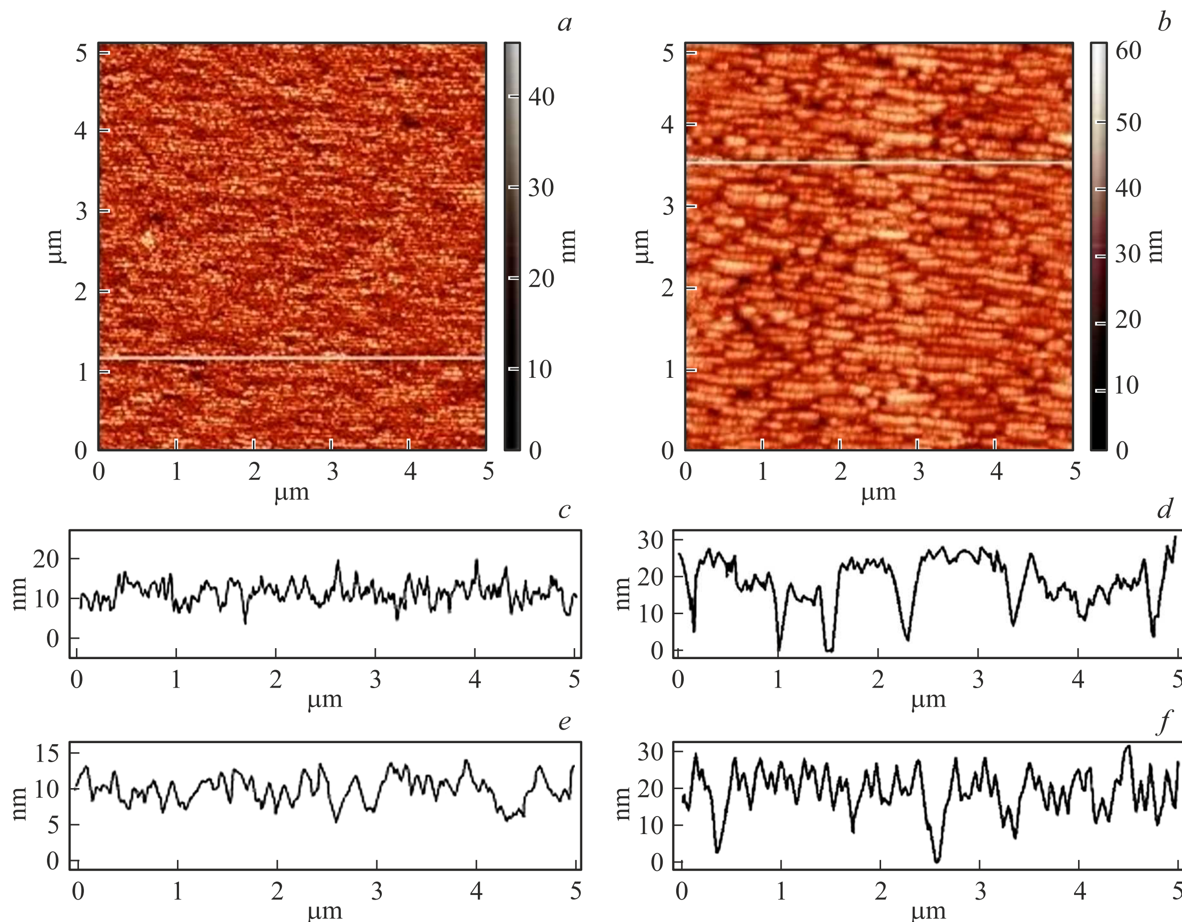

Figure 3. *a, b* — AFM images of structure surfaces; *c–f* — surface profiles in direction parallel to (*c, d*) and perpendicular to (*e,f*) direction of „nanogrooves": *a*, *c*, *e* — type „A", *b*, *d*, *f* — type „B".

the location of AIN and Si atoms is such that they are turned by 55° relative to each other. Phase-to-phase energy for cubic AlN on Si(100) and hexagonal AlN on cubic AlN must be lower than energy of hexagonal AlN on Si(100), therefore, hexagonal AlN on surface Si(100) is more preferable to be formed via cubic phase of AlN [18]. In virtue thereof, a thin texture layer of AlN, produced by RMS at low temperature, may contain both hexagonal and cubic phases, besides, cubic phase AlN will remain in the state of layer compression [18], which explains the maximum position of wide peak 661 cm^{-1}.

Growth of AIN layers by MOCVD method takes place at high $T \sim 1080°C$ temperature and causes formation of hexagonal layer only.

Surface of AIN layer in specimen „C" had a marked asymmetric nature inherent in blocks of semipolar aluminum nitride, which arise because of asymmetric properties of NP-Si(14) substrate after bombardment by ions N_2, as specified in cm [14]. Surface AFM demonstrated the difference in morphology of levels „A" and „B" (Fig. 3). The surface of layers in the direction parallel to „nanogrooves", is demonstrated by extended blocks. Dimensions of blocks in structures of „B" type are much larger than for „A": around 0.2 μm and 1–2 μm accordingly (Fig. 3, *c, d*). Height of blocks in structures „A" and „B" is 20 and 30 nm accordingly (Fig. 3, *c–f*). The difference is obviously related to a larger length of Al adatom range in direction of „nanogrooves" on the surface of AIN layer grown by RMS, compared to the length of adatom range directly on NP-Si(100) substrate. Indeed, the density of the broken bonds of nitrogen in the direction parallel to „nanogroove", is lower than in perpendicular direction, which causes difference in the lengths of diffusion along two directions of stepped surface. Application of buffer AIN layer reduces density of broken bonds on the surface of Np-Si(100), which supports migration of aluminum adatoms. It was noted that air cavities were formed upon origination of AIN layer by RMS method in areas of „nanogrooves"İhese cavities play a critical role in relaxation of tensions suppressing formation of cracks in upper layer of AlN.

Result: this paper obtained heteroepitaxial growth of AIN layers grown by MOCVD method on nanostructured Si(100) substrates with buffer AIN layer deposited by RMS method. In case of symmetric V-shaped nanogrooves on Si(100) surface on opposite side slopes in direction per-

pendicular to Si(111) face), in RMS method the asymmetric growth of block AlN layer occurs in the form of microbands with inclined surface. It is shown that the length of Al atom diffusion in direction parallel to „nanogroove", is higher than in perpendicular direction, which causes different dimensions of blocks along two directions of AlN-layer surface. Raman-scattering spectroscopy demonstrated that AlN/Si(100) template grown by RMS, is in a compression state, and AlN layer grown by MOCVD, had lower tension value compared to AlN layer obtained directly on NP-Si(100) substrate.

Acknowledgments

Authors would like to thank V.K. Smirnov for provision of NP-Si(100) substrates.

Conflict of interest

The authors declare that they have no conflict of interest.

References

[1] M. Kneissl, T.-Y. Seong, J. Han, H. Amano. Nat. Photonics, **13**, 233 (2019). DOI: 10.1038/s41566-019-0359-9
[2] Y. Liu, Y. Cai, Y. Zhang, A. Tovstopyat, S. Liu, C. Sun. Micromachines, **11**, 630 (2020). DOI: 10.3390/mi11070630
[3] M. Feng, J. Wang, R. Zhou, Q. Sun, H. Gao, Y. Zhou, J. Liu, Y. Huang, S. Zhang, M. Ikeda, H. Wang, Y. Zhang, Y. Wang, H. Yang. IEEE J. Sel. Top. Quantum Electron., **24**, 1 (2018). DOI: 10.1109/JSTQE.2018.2815906
[4] Y. Huang, J. Liu, X. Sun, X. Zhan, Q. Sun, H. Gao, M. Feng, Y. Zhou, M. Ikeda, H. Yang. Cryst. Eng. Comm., **22**, 1160 (2020). DOI: 10.1039/C9CE01677E
[5] Y. Sun, K. Zhou, M. Feng, Z. Li, Y. Zhou, Q. Sun, J. Liu, L. Zhang, D. Li, X. Sun, D. Li, S. Zhang, M. Ikeda, H. Yang. Light Sci. Appl., **7**, 13 (2018). DOI: 10.1038/s41377-018-0008-y.eCollection 2018
[6] Z. Zhang, J. Yang, D.-G. Zhao, F. Liang, P. Chen, Z.-S. Liu. Chin. Phys. B, **32**, 028101 (2023). DOI: 10.1088/1674-1056/ac6b2b
[7] T. Takeuchi, S. Sota, M. Katsuragawa, M. Komori, H. Takeuchi, H. Amano, I. Akasaki. Jpn. J. Appl. Phys., **36**, L382 (1997). DOI: 10.1143/JJAP.36.L382
[8] D. Rosales, B. Gil, T. Bretagnon, B. Guizal, F. Zhang, S. Okur, M. Monavarian, N. Izyumskaya, V. Avrutin, U. Ozgur, H. Morkoc, J.H. Leach. J. Appl. Phys., **115**, 073510 (2014). DOI: 10.1063/1.4865959
[9] W.G. Scheibenzuber, U.T. Schwarz, R.G. Veprek, B. Witzigmann, A. Hangleiter. Phys. Rev. B, **80**, 115320 (2009). DOI: 0.1103/PhysRevB.80.115320
[10] V.N. Bessolov, E.V. Konenkova. ZhTF, **93** (9), 1235 (2023) (in Russian). DOI: 10.21883/JTF.2023.09.56211.31-23
[11] Q. Feng, Y. Ai, Z. Liu, Z. Yu, K. Yang, B. Dong, B. Guo, Y. Zhang. Superlattices and Microstructures, **141**, 106493 (2020). DOI: 10.1016/j.spmi.2020.106493
[12] T. Yamada, T. Tanikawa, Y. Honda, M. Yamaguchi, H. Amano. Jpn. J. Appl. Phys., **52**, 08JB16 (2013). DOI: 10.7567/JJAP.52.08JB16
[13] I.-S. Shin, J. Kim, D. Lee, D. Kim, Y. Park, E. Yoon. Jpn. J. Appl. Phys., **57**, 060306 (2018). DOI: 10.7567/JJAP.57.060306
[14] V.N. Bessolov, E.V. Konenkova, S.N. Rodin, D.S. Kibalov, V.K. Smirnov. Semiconductors, **55** (4), 471 (2021). DOI: 10.1134/S1063782621040035
[15] V.N. Bessolov, N.D. Gruzinov, M.E. Kompan, V.N. Panteleev, S.N. Rodin, M.P. Shcheglov. Tech. Phys. Lett., **46** (4), 382 (2020). DOI: 10.1134/S1063785020040185
[16] V.N. Bessolov, E.V. Konenkova, T.A. Orlova S.N. Rodin, A.V. Solomnikova. Tech. Phys., **67** (5), 609 (2022). DOI: 10.21883/TP.2022.05.53677.12-22
[17] W. Zheng, R. Zheng, F. Huang, H. Wu, F. Li. Photon. Res., **3** (2), 38 (2015). DOI: 10.1364/prj.3.000038
[18] B. Riah, A. Ayad, J. Camus, M. Rammal, F. Boukari, L. Chekour, M.A. Djouadi, N. Rouag. Thin Solid Films, **655**, 34 (2018). DOI: 10.1016/j.tsf.2018.03.076

Translated by M.Verenikina